Prediction Of The Breast Tumour Based On Image Processing And Machine Learning Techniques

Ayat A. Yosif[1] , Haneen.altaie[2] , Alaa H.Jassim[3], Ameer Jawad Fadhl[4]

[1]College of Dentistry, University of Kerbala, Iraq, ayat.abdulalsada@uokerbala.edu.iq
[2]University of Kerbala, Iraq Haneen.abdulhussien@uokerbala.edu.iq
[3]University of Kerbala, Iraq alaa.hayder@uokerbala.edu.iq
[4]University of Kerbala, Iraq ameer.j@uokerbala.edu.iq

Abstract This study explored the prognostic value of a digital risk score (DRS) derived from computational analysis of breast tumor tissue images. A DRS model was developed and validated using a cohort of One thousand two hundred and ninety-nine patients with breast cancer were evaluated. The model showed good performance in detecting individual with higher risk pro-files. and low risk of breast cancer death based on tumor morphology, including size, grade, involvement of lymph nodes, and hormone receptor status. Survival analysis demonstrated significant predictive power of the DRS for both disease-specific and overall survival, particularly in specific tumor subtypes and Subgroups of hormone receptor status. The DRS exhibited a statistically significant difference in its prognostic model compared to a visual risk score assigned by experienced pathologists, highlighting the complementary nature of both approaches. Our findings suggest that the DRS, in conjunction with conventional clinicopathological factors, offers a valuable tool for risk stratification and personalized treatment guidance in breast cancer. This work used a machine learning algorithm trained on digital pictures of tumor tissue microarrays (TMAs) to build and validate a digital risk score (DRS) model for predicting patient survival, both overall and specific to breast cancer.

Kew words: Breast cancer, Digital risk score, Image analysis, Prognosis, Survival, Machine learning, Pathology.

1. Introduction

This article attempts to cover an extensive overview of one of the most prevalent women health problems all over the world-carcinoma of the breast. It also focuses on detecting such diseases at an early stage to enhance treatment and increase Longevity (Trapani et al., 2022). One of commonly used breast cancer early detection diagnostic imaging methods is the mammographic screening (Aristokli et al., 2022), however it has some limitations, such as high false-positive rate and the need of skilled radiological professional to interpret the results (Kim et al., 2020).Over the past few years, the focus has been on using image processing techniques and artificial neural networks Increase the accuracy of breast cancer diagnosis (Allugunti, 2022; Nomani et al., 2022; Zaylaa & Kourtian, 2024). The area with the recognition and appraisal of breast cancer could also benefit from machine learning in a way that fewer biopsies per patient could be required, and the overall diagnosis for each patient could be done more effectively (Witowski et al., 2022).

Machine learning algorithms used in personalized medicine systems utilize patients' medical records, their genetic profiles, and imaging information to make treatment recommendations (Alam, 2023). The integration of machine learning algorithms with image processing and Clinical Decision Support

Systems (CDSs) can assist healthcare practitioners in obtaining real-time diagnosis and treatment advice for patients (Sandeep Kumar & Satya Jayadev, 2020). Furthermore, advancements in explainable AI techniques will improve the explanation of AI models and increase trust in the outcomes predicted by machine learning or a diagnosis by a neural network (Zhang et al., 2022). The integration of images obtained from different imaging techniques, that is, multimodal imaging, could therefore provide knowledge and understanding of the disease of the malignant breast and result in higher diagnostic accuracies (Boehm et al., 2022; Jasti et al., 2022).

2. Materials and Methods

2.1. Microarrays of Tumor Tissue and Their Preparation for Patients

To conduct this study, researchers collected data from two sources: a national registry and a single hospital. The other dataset involved patients primarily diagnosed in the [region] area who received treatment at the [University Name] hospital by [date range from 2019 to 2023]. Both datasets contained detailed clinical and pathological information separated from hospital and research laboratory history. The study focused on analyzing data related to tumor characteristics such as type, grade, size, and the quantity of affected lymph nodes (Tavassoli & Devilee, 2003).

The study only included patients who had data on survival, including cause of death, digitized images of their breast neoplasm histology, and a sample of adequate size (greater than 0.02 mm^2, corresponding to 400,000 pixels of image resolution) (Joensuu et al., 2003).

2.2. Image Acquisition

Very thin slices (5 micrometers) were obtained from the TMA blocks. These slices were then stained using a standard technique (hematoxylin and eosin) and scanned digitally using a high-powered slide scanner (Pannoramic 250 FLASH). The scanner has a strong magnifying lens (20x objective) and uses a special camera to capture the image. This camera has three separate light sensors that capture high-resolution images (1618 x 1236 pixels). Each pixel in the final image corresponds to a tiny area of the tissue (0.22 x 0.22 micrometers).

2.3. Outcome Classification and Digital Risk Score

We employed a sophisticated technique called "Improved Fisher Vector Encoding" (IFV) to analyze the TMA spot images. IFV extracts informative details from each image using a pre-trained deep learning model (VGG-16). These details are then condensed into a single descriptor, allowing the model to handle images of varying sizes. Studies have shown that IFV can be more effective than relying solely on the model's final layers for image analysis. Patients who succumbed to Those who died of breast carcinoma within 10 years of diagnosis were categorized as high risk (N=340). Conversely, individuals who survived until the end of the follow-up time period were classified as low risk (N=528). Finally, the Support Vector Machine (SVM) algorithm was established with 868 tissue microarray (TMA) images of breast cancer (each image represented a case of a patient) (Cimpoi et al., 2015; Vedaldi & Lenc, 2015).

2.4. Visual risk scoring

Three independent pathology experts reviewed the TMA spot images from the test set using an online site for image viewing and annotating. They then stratified the samples as cancer-predisposing or non-cancer-predisposing samples. > In the foils of to to 10% of the cats images - All judges or evaluators reached a consensus (had a unified view).Exploring Chitosan's Potential as a Bio-Based Adsorbent for Sustainable Aflatoxin Mitigation. Furthermore, a single pathologist assessed specific characteristics within each TMA spot, including: the number of mitoses (categorized as 0, 1, or more

than 1), the level of pleomorphism (minimal, moderate, or marked), the percentage of tubules (≤10%, 10%–75%, or >75%), presence or absence of necrosis, and TILs (sparse or abundant).

2.5. Statistical analysis

To estimate the probability of surviving for a specific time (survival function), researchers employed the Kaplan-Meier method. This technique was then used to compare The log-rank test was used to compare separate survival curves. Disease-specific survival (DSS) is defined as the time from the first diagnosis until death as a result of breast cancer only. Patients who were alive at the end of the study or who died from causes other than gastric cancer were excluded (censored) from the DSS analysis. On the other hand, as opposed to PFS, which ranges from the time of diagnosis until disease-related death and surviving patients at the time-point of the study were also omitted from the analysis, overall survival (OS) includes time from diagnosis until death independently of the cause were included survivors at the time-point of the study is also excluded from the analysis (Kaplan & Meier, 1958).

3. Results

3.1 Outcome classification

To develop a digital risk score (DRS) model, we trained a classifier algorithm on a dataset of 868 tumor tissue images. Next, a different exam set consisting of 430 patient role with breast cancer were classified This procedure was used to classify subjects into low or high risk groups. When assessing the test-set 55% (237 individuals) as low-risk and 45% (194 individuals) as high-risk (see Table 1 for details). The performance of the algorithm was evaluated by the AUC. The AUC value achieved in our study was consistent between the training and testing cohort (0.63, 0.58, respectively), which means the performance of model was high generalized and had avoided overfitting.

3.2. Classification of outcomes and clinicopathological factors

Participants classified at high risk of dying from breast cancer had adverse tumor characteristics (Table 1). This subgroup had significantly higher rates of high-risk tumors ($p = 0.014$) than those which were classified as low-risk. Furthermore, the tumors from the high-risk population were significantly larger in size ($p < 0.001$), had more lymph node involvement ($p = 0.003$), and a higher proportion of progesterone receptor-negative cases ($p = 0.015$). Digital risk assesment and visual risk assessment measurements have a strong association with tumor histopathologic features (see Supplementary Table 1). The DRS was specifically associated with nuclear atypia and tubular formation.

Table 1: Features of the patient

Changeable	Whole data set (N = 1299)				p Value	Test set (N = 431)				p Value
	Exercise set (N = 868)		Exercise set (N = 431)			LowDRS (N=237)		High DRS (N = 194)		
	%	N	%	N		%	N	%	N	
The quantity of lymph nodes that are positive										
Mean	1.4		1.2		0.407	0.9		1.6		**0.003**
0	58	504	59	253	0.323	63	150	53	103	**0.057**
1–3	24	206	23	99		23	54	23	45	

4–9	8	73	9	38		6	15	12	23	
>10	3	30	2	7		1	2	3	5	
Unknown	6	55	8	34		7	16	9	18	
Tumour size (mm)										
Mean	23.7		23.2		0.817	2.15		25.3		**<0.001**
Unknown	3.0	28	5.0	22		5	13	5	9	
Histological grade										
I	16	143	19	83	0.086	23	54	22	43	**0.014**
II	34	296	36	154		32	75	41	79	
III	23	197	18	76		14	33	22	43	
Unknown	27	232	27	118		32	75	22	43	
Histological type										
Ductal	76	662	77	333	0.742	74	175	81	158	**0.079**
Lobular/special	24	206	23	98		26	62	19	36	
Age										
≤39	7	63	7	30	0.353	9	21	5	9	**0.140**
40–49	21	186	24	103		27	64	20	39	
50–59	27	234	22	94		21	49	23	45	
60–69	20	172	21	91		20	47	23	44	
≥70	25	213	26	113		24	56	29	57	
ER										
Negative	29	248	27	116	0.572	25	60	29	56	**0.443**
Positive	62	538	64	274		65	155	61	119	
Unknown	9	82	10	41		9	22	10	19	
PR										
Negative	42	362	41	177	0.803	36	86	47	91	**0.015**
Positive	49	423	50	215		56	132	43	83	
Unknown	10	83	9	39		8	19	10	20	
HER2										

Negative	72	623	74	321	0.713	76	181	72	140	**0.136**
Positive	17	146	16	70		14	32	20	38	
Unknown	**11**	**99**	**9**	**40**		**10**	**24**	**8**	**16**	

The investigation looked at relationships between patient data and clinicopathological variables. While the right panel compares patients classified into low and high digital risk score (DRS) categories, the left panel displays these connections within the training and test sets. Results that are statistically significant (p-value < 0.05) are bolded.

3.3 Classification of outcomes, visual risk assessment, and digital risk assessment

In the univariate analysis, the digital risk score appeared as a statistically significant marker of DSS with a hazard ratio (HR) of 2.10 (95% confidence interval [CI] 1.40–3.18, p < 0.001) and a concordance index (C-index) of 0.60 (95% CI 0.55–0.65). The visual risk assessment was also found to be a significant prognostic factor with a HR of 1.74 (95% CI: 1.16 – 2.61, p = 0.006) and a C-index of 0.58 (95% CI: 0.53 – 0.63). (see Supplementary Fig. 1 and Fig. 2). It's interesting to note that a Chi-squared test of the individual survival models between species showed a highly significant

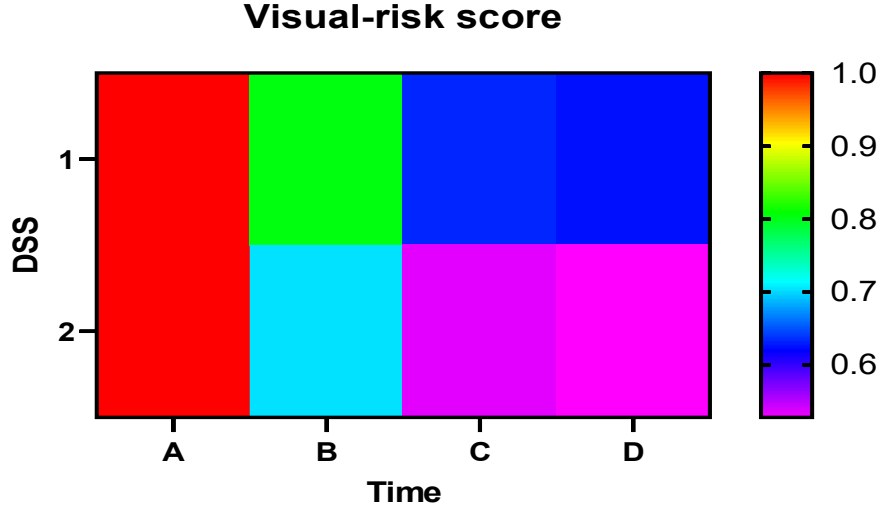

difference between both of them (p < 0.001). In multivariable survival analysis, the visual risk classification and the benchtop risk score (DRS) category were identified as independent prognostic factors with a hazard ratio of 2.05 (p < 0.001). DRS (p < 0.003 disc area) and HR = 1.68, p = 0.012, for the visual risk classification. The joint survival model attained a concordance index of 0.64 (95% confidence interval:0.58-0.69).

Fig. 1: The heat map shows disease-specific survival (DSS) categorized as low or high Visual-risk score.

3.4 Classification and survival analysis

This study assessed the DRS grouping's ability to predict survival outcomes for breast cancer patients in the test set. We used both single-variable and multivariable analytic approaches. The study found that women with low DRS had a higher chance of survival, including Survival results for breast cancer (p < 0.001) and overall mortality (p = 0.003) were found to be significantly different (Figures 1 and

2). The 10 year disease-specific survival probability of low DRS category versus elevated DRS category was 82% (95% CI 77–87%) and 65% (95% CI 58–73%), respectively.

The dataset was then split according to grade of histological grading, as reported of the original whole-slide tissue samples. Categorization by digital risk score (DRS) showed the most possible precision for detection of grade I tumors ($p < 0.001$). However, differences in grade II ($p = 0.410$) and grade III ($p = 0.083$) did not reach statistical significance. Importantly, DRS model remained a strong prognostic factor for survival in both ER-positive ($p = 0.025$) and ER-negative ($p < 0.001$) patient groups. Furthermore the DRS adjusted stratification had no longer a significant distinguished sufficient. predictor in the PR-negative subgroup, but not in the PR-positive subgroup ($p = 0.003$). The classification by DRS was also an independent prognostic factor for HER2-negative ($p = 0.015$) and HER2-positive ($p < 0.001$) patients (Table 2). Subgroup analysis based on tumor size and lymphatic metastasis is shown (see Figure 4).

Hazard ratio (HR) = 2.04, 95% CI: 1.20–3.44, $p = 0.007$) After adjusted by multivariable survival model, patients belonging to high-risk category of DRS was associated with worse clinical outcomes, as an independent prognostic marker (see Table 2). In addition, tumor size (HR = 1.04, 95% CI: 1.02–1.06, $p < 0.001$), progesterone receptor-positive (HR = 0.42, 95% CI: 0.25–0.71, $p < 0.001$), and more than 10 metastatic lymph nodes (HR = 4.74, 95% CI: 1.17–19.30, $p = 0.029$) were observed as independent factors associated with survival.

Table2: Performing Cox uni- and multivariate survival analyses.

Variables	Univariate analysis			Analyzing several variables		
	H. R	95% of CI	p value	H. R	94% of CI	p Value
DRS						
Low	Rf			Rf		
High	2.10	1.33:3.32	**0.001**	2.04	1.20:3.44	**0.007**
Quantity of favorable lymph nodes						
0	Rf			Rf		
1–3	1.53	(0.89—2.63)	0.123	2.12	(0.83–1.47)	**0.116**
4–9	2.93	(1.61–5.33)	**0.001**	2.15	(0.75–6.19)	**0.154**
>10	7.43	(2.90–19.02)	**0.001**	4.75	(1.17–19.30)	**0.029**
Size of the tumour						
by mm	1.04	1.030:1.060	**0.001**	1.04	1.020:1.060	**0.001**
Grade histologically						
1	Rf			Rf		
2 or 3	3.14	1.61:6.09	**0.001**	1.57	0.76:3.20	**0.220**
Histological kind						
Ductal	Rf			Rf		
Lobular/special	0.73	0.40:1.33	0.30	0.90	0.41:1.95	**0.781**
Age						
≤ 39	Rf			Rf		
40: 49	0.78	0.33:1.88	0.57	0.42	0.17:1.12	**0.083**
50: 59	0.69	0.28:1.8	0.42	0.48	0.19:1.27	**0.143**
60: 69	1	0.42:2.35	0.98	0.61	0.25:1.58	**0.318**

≥70	1.58	0.66:3.79	0.30	1.35	0.49:3.72	**0.563**
ER						
Negative	Ref.					
Positive	0.69	(0.44–1.09)	0.15			
PR						
Undesirable	Rf			Rf		
Optimistic	0.34	0.21:0.55	**0.001**	0.42	0.25–0.71	**0.001**
HER2						
Undesirable	Rf					
Optimistic	1.51	0.90:2.53	0.119	1.07	0.57–1.99	**0.831**
Systematic treatment.						
Not provided	Rf			Rf		
Given	1.90	1.21:2.98	**0.005**	1.07	0.22:1.47	**0.244**
Local therapy						
Undesirable	Rf			Rf		
Assumed	**1.24**	**0.75:2.03**	**0.404**	**1.22**	**(0.61:2.46**	**0.57**

To analyze tumor characteristics, we examined whole tissue sections for microtumor categorization and subtyping. ER status, progesterone receptor (PR) status, and HER2 expression (HER2) gene amplification were assessed using tissue microarrays (TMAs). Because ER data did not fulfill statistical assumptions, it was removed from the multivariate analysis.

Fig. 2: Disease-specific survival (DSS) is dichotomized by low/high digital risk score. Data are presented as mean ± SE (n = 3). Asterism on top of the bars in the graph was used to show statistically significant differences between test and control groups: for p < 0.05, * for p < 0.01, etc. 0.001 (***), and p < 0.0001 (****).

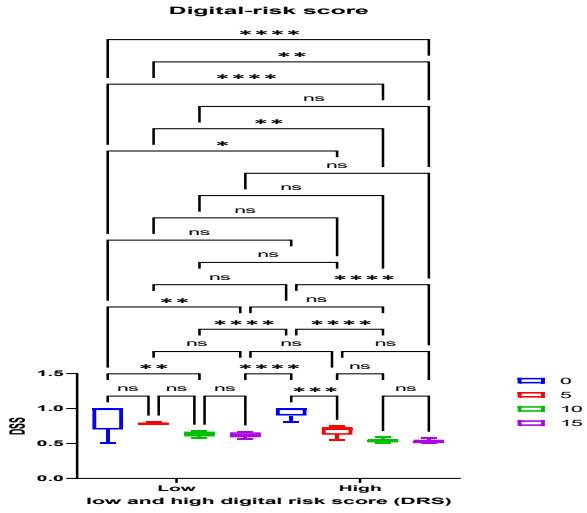

4. Discussion

This study aimed to explore the utility of a digital risk score (DRS), derived from computer analysis of breast tumor tissue images, as a prognostic tool for breast cancer patients. Our findings suggest that the DRS holds significant promise in augmenting traditional clinicopathological assessments and providing valuable insights into long-term survival outcomes.

The first pivotal observation of our study was the DRS model's ability to effectively differentiate between patients exhibiting a high and low risk of breast cancer death. In accordance with this, it is crucial to point out the presence of a rather profound difference between two risk groups regarding the tumor profile features. Notably, as per the high-risk group, there occurred higher proportions of sample tumors of high grade, larger size, and increased nodes and a higher likelihood of not being progesterone receptor-positive (Davey et al., 2021). These outcomes can be explained by the fact that thanks to the awareness of BC and its signs, when regarding the aggressiveness of the tumor characteristics, higher values characterize worse outcomes for the patient (Scimeca et al., 2019). These morphological changes are / are significant and intricate but the DRS model with the help of the image analysis derived from such vital morphological markers gave a quantifiable risk score (Bi et al., 2019). This is due to the fact that this incredible utility hails from the improvement of the Fisher vector method (FV) known as improved Fisher vector (IFV) alongside the VGG-16 deep learning model (Kamaleldin et al., 2023). These methods helped the DRS to get better and finer information of images, which cannot be determined by the naked eye.

Comparing the result of the study in the particular concerns of survival and on some of the survival-oriented questions used in the study, it is evident that the DRS model possesses good predictive capability when utilized for prognosis. In this study, the results showed that the DRS, low risk patients' survival probability was highly considerate compared to high-risk counterpart patients. (Katz et al., 2018; Martín Vicario et al., 2024). Strikingly, the DRS's performance differed across different tumor types as to their prognostic strengths. It showed the best predictive ability for grade I tumors and proved that some degree of clinical discrimination may be possible if cancer subtypes with specific features are included in the analysis (Łukasiewicz et al., 2021; Schneider & Langner, 2014). DRS could also predict the outcome in sub-groups defined by the ER status and the PR status of the patients. The authors showed that DRS was a predictor in ER positive and negative patients but it was not predictive in the PR-positive and PR-negative patients (Habibi et al., 2008). These results thus bring to the fore the need to integrate the DRS with other clinicopathological features of the tumor before making an individual prognosis of a patient.

This study also dedicated a part of the methodology to the comparison between the DRS and the visual risk score which was assigned by an expert pathologist based on the analysis of the same tumor images. (Aeffner et al., 2017, Turkki et al., 2019). Every difference mentioned in this distinct focus underlines the fact that Scoring Systems are alternative. The DRS presents that features based on objective morphological criteria, while VRS is a qualitative rapid estimation that factors a lot of subjective information from the pathologist's knowledge (Turkki et al., 2019). By developing the aforementioned approaches further for a multi-variate analysis, the team came out with a better prognostic model and inferred the need for providing a solution with overtakes the digital health practitioner. The DRS's increased potential to improve the prediction of post-surgery survival results, beyond the conventional clinicopathological assessment, offers the possibility for more personalized treatments and also allows for better patient counseling and risk stratification (Kenner et al., 2021). This can result in drugs being offered more specifically, increased management of disease progression, and improved outcomes for patients (Guest et al., 2020). However, what should also be pointed out is that there are particular restrictions regarding this type of research. Thus, developments such as retrospective design, the selected patient population, and a relatively small research sample suggest that such findings should be replicated in subsequent studies with bigger and more diverse samples of participants (Targher et al., 2016). Future research should focus on the organization of the DRS in the clinic, cost-effectiveness analysis of the DRS, and the DRS-based individualized differential treatment strategies.

Therefore, in summing up, the research foresees a bright future for the DRS as an effective forecasting marker in breast cancer. A new trend in the assessment of tumor tissues has however been added by

the utilization of image analysis technologies that are advanced in an endeavor to extract useful information from the images of tumor tissues in supplement to the conventional clinicopathological means (Hamilton et al., 2014). Thus, while the present findings provide some evidence regarding the potential of the DRS to help with individualized risk assessment and accurate counselling about prognosis and possible treatments.

5. conclusion

The study focuses on investigating how a digital risk score calculated from breast tumor images can be used to classify tumors and predict long-term prognosis in breast cancer patients. It also emerges that the DRS add significant prognostic information to the conventional clinicopathological factors and have strong predictive power especially in specific tumors subtype and HR negativity. It is able to emphasize the visual risk scores evaluated by professional pathologists in a discriminating manner and provides a complementary way for the risk prediction. DRS may have the potential for individualized treatment regimens, better management of acute and chronic disease, and improved outcomes. But it is yet unclear if it can be reliably used in clinical practice and adapted to larger populations/cases and whether it is cost-effective. The combination of sophisticated image processing tactics and computational strategies has a potential to fundamentally transform the field of oncological diagnosis and prediction.

References

1. Abdulrazzaq, A. A., Muhammed, Y., Al-Douri, A. T., Mohamad, A., & Ibrahim, A. M. (2022). Automatic Segmentation of Calcification Areas in Digital Breast Images. BioMed Research International, 2022.
2. Aeffner, F., Wilson, K., Martin, N. T., Black, J. C., Hendriks, C. L. L., Bolon, B., Rudmann, D. G., Gianani, R., Koegler, S. R., & Krueger, J. (2017). The gold standard paradox in digital image analysis: manual versus automated scoring as ground truth. Archives of pathology & laboratory medicine, 141(9), 1267-1275.
3. Alam, S. (2023). PMTRS: A Personalized Multimodal Treatment Response System Framework for Personalized Healthcare. International Journal of Applied Health Care Analytics, 8(6), 18-28.
4. Allugunti, V. R. (2022). Breast cancer detection based on thermographic images using machine learning and deep learning algorithms. International Journal of Engineering in Computer Science, 4(1), 49-56.
5. Aristokli, N., Polycarpou, I., Themistocleous, S., Sophocleous, D., & Mamais, I. (2022). Comparison of the diagnostic performance of Magnetic Resonance Imaging (MRI), ultrasound and mammography for detection of breast cancer based on tumor type, breast density and patient's history: A review. Radiography, 28(3), 848-856.
6. Balkenende, L., Teuwen, J., & Mann, R. M. (2022). Application of deep learning in breast cancer imaging. Seminars in Nuclear Medicine,
7. Bi, W. L., Hosny, A., Schabath, M. B., Giger, M. L., Birkbak, N. J., Mehrtash, A., Allison, T., Arnaout, O., Abbosh, C., & Dunn, I. F. (2019). Artificial intelligence in cancer imaging: clinical challenges and applications. CA: a cancer journal for clinicians, 69(2), 127-157.
8. Boehm, K. M., Khosravi, P., Vanguri, R., Gao, J., & Shah, S. P. (2022). Harnessing multimodal data integration to advance precision oncology. Nature Reviews Cancer, 22(2), 114-126.
9. Chen, H., & Shi, Z. (2020). A spatial-temporal attention-based method and a new dataset for remote sensing image change detection. Remote Sensing, 12(10), 1662.
10. Dhall, D., Kaur, R., & Juneja, M. (2020). Machine learning: a review of the algorithms and its applications. Proceedings of ICRIC 2019: Recent innovations in computing, 47-63.
11. Guest, F. L., Rahmoune, H., & Guest, P. C. (2020). Early diagnosis and targeted treatment strategy for improved therapeutic outcomes in Alzheimer's disease. Reviews on New Drug Targets in Age-Related Disorders, 175-191.
12. Habibi, G., Leung, S., Law, J. H., Gelmon, K., Masoudi, H., Turbin, D., Pollak, M., Nielsen, T. O., Huntsman, D., & Dunn, S. E. (2008). Redefining prognostic factors for breast cancer: YB-1 is a stronger predictor of relapse and disease-specific survival than estrogen receptor or HER-2 across all tumor subtypes. Breast Cancer Research, 10, 1-9.

13. Hamilton, P. W., Bankhead, P., Wang, Y., Hutchinson, R., Kieran, D., McArt, D. G., James, J., & Salto-Tellez, M. (2014). Digital pathology and image analysis in tissue biomarker research. Methods, 70(1), 59-73.
14. Targher, G., Byrne, C. D., Lonardo, A., Zoppini, G., & Barbui, C. (2016). Non-alcoholic fatty liver disease and risk of incident cardiovascular disease: a meta-analysis. Journal of hepatology, 65(3), 589-600.
15. Tavassoli, F. A., & Devilee, P. (2003). Pathology and genetics. World Health Organization Classification of Tumours: Tumours of the Breast and Female Genital Organs. Washington, DC: International Agency for Research on Cancer.
16. Trapani, D., Ginsburg, O., Fadelu, T., Lin, N. U., Hassett, M., Ilbawi, A. M., Anderson, B. O., & Curigliano, G. (2022). Global challenges and policy solutions in breast cancer control. Cancer treatment reviews, 104, 102339.
17. Turkki, R., Byckhov, D., Lundin, M., Isola, J., Nordling, S., Kovanen, P. E., Verrill, C., von Smitten, K., Joensuu, H., & Lundin, J. (2019). Breast cancer outcome prediction with tumour tissue images and machine learning. Breast cancer research and treatment, 177, 41-52.
18. Vedaldi, A., & Lenc, K. (2015). Matconvnet: Convolutional neural networks for matlab. Proceedings of the 23rd ACM international conference on Multimedia,
19. Witowski, J., Heacock, L., Reig, B., Kang, S. K., Lewin, A., Pysarenko, K., Patel, S., Samreen, N., Rudnicki, W., & Łuczyńska, E. (2022). Improving breast cancer diagnostics with deep learning for MRI. Science translational medicine, 14(664), eabo4802.
20. Yang, W., Wang, W., Huang, H., Wang, S., & Liu, J. (2021). Sparse gradient regularized deep retinex network for robust low-light image enhancement. IEEE Transactions on Image Processing, 30, 2072-2086.
21. Younis, Y. S., Ali, A. H., Alhafidhb, O. K. S., Yahia, W. B., Alazzam, M. B., Hamad, A. A., & Meraf, Z. (2022). Early diagnosis of breast cancer using image processing techniques. Journal of Nanomaterials, 2022, 1-6.
22. Zaylaa, A. J., & Kourtian, S. (2024). Advancing Breast Cancer Diagnosis through Breast Mass Images, Machine Learning, and Regression Models. Sensors, 24(7), 2312.
23. Zhang, Y., Weng, Y., & Lund, J. (2022). Applications of explainable artificial intelligence in diagnosis and surgery. Diagnostics, 12(2), 237.
24. Zubair, M., Wang, S., & Ali, N. (2021). Advanced approaches to breast cancer classification and diagnosis. Frontiers in Pharmacology, 11, 632079.